Machine Intelligence Research
www.mi-research.net

20(5), October 2023, 697-706
DOI: 10.1007/s11633-022-1345-0

ECG Biometrics via Enhanced Correlation and Semantic-rich Embedding

Kui-Kui Wang[1] Gong-Ping Yang[1,2] Lu Yang[3] Yu-Wen Huang[2] Yi-Long Yin[1]

[1]School of Software, Shandong University, Jinan 250101, China

[2]School of Computer, Heze University, Heze 274015, China

[3]School of Computer Science and Technology, Shandong Jianzhu University, Jinan 250101, China

Abstract: Electrocardiogram (ECG) biometric recognition has gained considerable attention, and various methods have been proposed to facilitate its development. However, one limitation is that the diversity of ECG signals affects the recognition performance. To address this issue, in this paper, we propose a novel ECG biometrics framework based on enhanced correlation and semantic-rich embedding. Firstly, we construct an enhanced correlation between the base feature and latent representation by using only one projection. Secondly, to fully exploit the semantic information, we take both the label and pairwise similarity into consideration to reduce the influence of ECG sample diversity. Furthermore, to solve the objective function, we propose an effective and efficient algorithm for optimization. Finally, extensive experiments are conducted on two benchmark datasets, and the experimental results show the effectiveness of our framework.

Keywords: Biometrics, matrix factorization, electrocardiogram (ECG), semantic information, enhanced correlation.

Citation: K. K. Wang, G. P. Yang, L. Yang, Y. W. Huang, Y. L. Yin. ECG biometrics via enhanced correlation and semantic-rich embedding. *Machine Intelligence Research*, vol.20, no.5, pp.697–706, 2023. http://doi.org/10.1007/s11633-022-1345-0

1 Introduction

Recent years have witnessed the surge of biometrics, such as fingerprints, faces, irises, and voices. Electrocardiogram (ECG) is also regarded as an inherent liveness biometric trait[1] with the advantage of being captured from a living individual. Most pioneering methods are designed to extract discriminative features from ECG signals based on fiducial or non-fiducial. For example, 19 stable fiducial features[2] related to interval, amplitude, and angle were computed from each heartbeat. The non-fiducial methods usually used wavelet features[3], statistical features, or autocorrelation (AC) features[4, 5]. Besides, several works with sparse representation[6–8] and dimensionality reduction, e.g., principal component analysis (PCA), kernel PCA (KPCA), linear discriminant analysis (LDA)[9–11], have also shown the success in ECG biometrics.

Although previous research works have gained promising performance, one limitation is that the existing methods cannot comprehensively exploit the diverse information among the ECG. During the collection, ECG signals are easily affected by changes in physiological and psychological activity, such as emotional factors, diets, diseases, electrode position, and other factors[12], causing the diversities between heartbeats of homologous samples to be large while heterologous samples are smaller. Hence, it is necessary to alleviate the impact of diversity and learn a discriminative feature representation to improve the recognition performance.

Motivated by the success of matrix factorization in other tasks, several promising methods[13, 14] based on matrix factorization for ECG biometrics have been proposed. Wang et al.[15] proposed a multi-scale differential feature with collective matrix factorization to generate a robust ECG representation. Li et al.[16] opted graph regularized non-negative matrix factorization and sparse representation to obtain non-fiducial features. Huang et al.[17] designed a multi-feature collective non-negative matrix factorization model. However, most matrix factorization methods for ECG biometrics aim to learn the latent discriminative representation without fully exploring the correlation between the base feature and latent representation to alleviate the impact of sample diversity.

In this paper, we focus on exploring the ECG sample diversity by taking advantage of matrix factorization to learn a latent representation. There are two problems to be considered. The first is how to minimize the sample diversity to improve recognition performance and the second is how to construct a strong correlation between the base feature space and the latent space to enhance

Research Article
Manuscript received on April 6, 2022; accepted on June 6, 2022; published online on January 11, 2023
Recommended by Associate Editor Cheng-Lin Liu
Colored figures are available in the online version at https://link.springer.com/journal/11633

the discriminative capability of learned representation.

To handle the above issues, we propose a novel framework, termed enhanced correlation and semantic-rich embedding matrix factorization for ECG biometrics. In specific, to acquire similar representations for homologous samples of the same subject and push away the representations of heterologous samples from different subjects, we introduce the pairwise similarity among all samples into our framework. For deep mining and accurately embedding of the intrinsic information of the base feature, we construct an enhanced correlation between the base feature and the latent representation. To further enhance the discriminative capability of the learned representation, we make orthogonal constraints on it. Finally, a novel optimization algorithm is proposed to learn our model. The main contributions of this paper are summarized as follows:

1) A new framework is proposed to effectively learn the latent representation of ECG signals. In this framework, pairwise similarity, label vectors, and base features work seamlessly and collectively to ensure high-quality latent representation.

2) To optimize the proposed novel objective function, an effective learning algorithm is presented. Through this algorithm, we could accurately and quickly solve the loss function.

3) We perform extensive experiments on two benchmark datasets and the experimental results demonstrate the effectiveness of our method.

The remainder of this paper is organized as follows. Related work is presented in Section 2. The details of our proposed method and matching procedure are presented in Section 3. Section 4 shows the experimental results and the conclusions are presented in Section 5.

2 Related work

ECG is a physiological signal generated from the contraction and the recovery of the heart. Generally, there are two main types of ECG acquisition settings for ECG biometrics, i.e., on-the-person and off-the-person. On-the-person acquisition usually uses multiple electrodes attached to the skin surface, such as medical datasets MIT-BIH arrhythmia database (MIT-BIH)[18]. For off-the-person datasets, they usually acquire ECG signals using dry button electrodes held by the subjects in contact with their finger, wrist, and so on, such as check your biosignals here initiative (CYBHiDB)[19]. Specifically, off-the-person acquisition addresses the reduced acceptability and comfort, and it has lower signal-to-noise ratios, which means considerably more noise influence.

The ECG signal is a cyclic repetition of five fiducial points, i.e., P, Q, R, S, and T waves. And the existing ECG biometric recognition methods can be roughly divided into three categories, i.e., fiducial methods, non-fiducial methods, and deep learning-based methods. For the fiducial methods, features are extracted employing the fiducial points of heartbeat, such as amplitudes, time duration, QRS complex, angles, slopes, areas, etc. Some methods[20–25] extract a class of features from dominant fiducial points of the ECG waveform. Non-fiducial methods do not use the fiducial points to generate the feature set, but focus on the whole signal or segmented by a sliding window. Some previous works have shown the success using the Gaussian model[26], statistical features[27], one-dimensional multi-resolution local binary patterns (1DMRLBP)[28], discrete wavelet transformation (DWT), and kernel methods[29] to extract non-fiducial features.

With the popularity of deep neural networks, some pioneer works[30, 31] adopting DNN for effective feature representations, have been proposed. Salloum and Kuo[32] adopted the LSTM-based RNN for ECG biometrics without any feature extraction. Zhao et al.[33] integrated a generalized S-transformation and CNN for human identification. Labati et al.[34] extracted significant features from one or more leads using a deep CNN. Especially, deep learning-based models can directly deal with ECG signals with blind segmentation rather than handcrafted features, and they can perform significantly better than most non-deep methods. However, most of them are time-consuming and lack interpretability. Thus, we mainly focus on how to efficiently refine the reliable base feature for ECG biometrics in our paper.

3 Proposed method

3.1 Notations

Assuming that the training set is formed by n samples, the base feature extracted from the ECG signal is represented by $\boldsymbol{X} = [\boldsymbol{x}_1, \boldsymbol{x}_2, \cdots, \boldsymbol{x}_n] \in \mathbf{R}^{m \times n}$, where m is the dimensionality of the base feature space. $\boldsymbol{L} \in \{1, 0\}^{c \times n}$ is the label matrix, where c is the number of subjects. $\boldsymbol{L}_{i,j} = 1$ if the j-th sample belongs to the i-th subject and $\boldsymbol{L}_{i,j} = 0$ means the opposite. $\|\cdot\|_F$ is the Frobenius norm, and $\boldsymbol{I}$ denotes an identity matrix.

3.2 Constructing enhanced correlation

Given the base feature matrix $\boldsymbol{X}$, we want to refine it to learn more powerful representations. The most intuitive way is to use the matrix factorization technique to remove the redundant information in $\boldsymbol{X}$ and provide the low-rank vectorial representations. We can formulate the operation as follows:

$$\min_{\boldsymbol{P_V}, \boldsymbol{V}} \|\boldsymbol{X} - \boldsymbol{P_V}\boldsymbol{V}\|_F^2 + \eta \|\boldsymbol{P_V}\|_F^2 \tag{1}$$

where $\boldsymbol{V}$ is the latent representation matrix, $\|\boldsymbol{P_V}\|_F^2$ is regularization term, and η is a trade-off parameter that controls it.

Meanwhile, we could learn a projection matrix $\boldsymbol{P_X}$ to map the original base feature to the latent $\boldsymbol{V}$, and the following formulation can be derived as

$$\min_{\boldsymbol{P_X},\boldsymbol{V}} \|\boldsymbol{V}-\boldsymbol{P_X}\boldsymbol{X}\|_F^2+\eta\|\boldsymbol{P_X}\|_F^2. \tag{2}$$

By combining the above two equations, we could extract more information from $\boldsymbol{X}$ and learn a more accurate $\boldsymbol{V}$, and the idea is similar to the auto-encoder. Here, to enhance the recognition ability, we let $\boldsymbol{P_X}=\boldsymbol{P_V^{\mathrm{T}}}$ and denote the projection matrix as $\boldsymbol{P}$. Then, the optimization problem is formulated as

$$\min_{\boldsymbol{P},\boldsymbol{V}} \theta\|\boldsymbol{V}-\boldsymbol{P}\boldsymbol{X}\|_F^2+\delta\left\|\boldsymbol{X}-\boldsymbol{P}^{\mathrm{T}}\boldsymbol{V}\right\|_F^2+\eta\|\boldsymbol{P}\|_F^2 \tag{3}$$

where θ and δ are trade-off parameters and the projection $\boldsymbol{P}$ is an enhanced correlation between the base feature and the latent representation.

3.3 Preserving semantic-rich information

The diversity of ECG signals is a primary factor affecting the recognition performance, and how to capture more semantic information is another essential problem.

Undoubtedly, homologous samples of the same subject should have as similar latent representations as possible, while the representations of heterologous samples from different subjects should be pushed away. To fulfill this purpose, we first define the pairwise similarity among all samples from label information $\boldsymbol{S}=\boldsymbol{G}^{\mathrm{T}}\boldsymbol{G}$ and $\boldsymbol{G}$ is a 2-norm column normalized label matrix, with its j-th column defined as $\boldsymbol{G}_{*j}=\boldsymbol{L}_{*j}/\|\boldsymbol{L}_{*j}\|$. Notably, we do not generate $\boldsymbol{S}$ in advance and directly use it in optimization because its size is $n\times n$ which may cause large complexity. However, for a better understanding of our paper, we still use $\boldsymbol{S}$ in the following. With the defined similarity matrix, we could use the inner product to preserve it with latent representations:

$$\min_{\boldsymbol{V}} \|\boldsymbol{S}-\boldsymbol{V}^{\mathrm{T}}\boldsymbol{V}\|_F^2 \tag{4}$$

which has a symmetric form with respect to $\boldsymbol{V}$.

Then, we intend to move a step further towards preserving semantic-rich information. Similarly, the matrix factorization technique helps

$$\min_{\boldsymbol{V},\boldsymbol{W}} \left\|\boldsymbol{V}-\boldsymbol{W}^{\mathrm{T}}\boldsymbol{L}\right\|_F^2 \tag{5}$$

where $\boldsymbol{W}$ is the projection matrix, and $\boldsymbol{L}$ is the label matrix. The above equation means that the learned latent representation could contain the information of the label matrix.

As both (4) and (5) try to preserve the semantic information of samples, we try to reformulate them into one equation:

$$\min_{\boldsymbol{V},\boldsymbol{W}} \alpha\left\|\boldsymbol{S}-\boldsymbol{V}^{\mathrm{T}}\boldsymbol{W}^{\mathrm{T}}\boldsymbol{L}\right\|_F^2+\beta\left\|\boldsymbol{V}-\boldsymbol{W}^{\mathrm{T}}\boldsymbol{L}\right\|_F^2+\gamma\|\boldsymbol{W}\|_F^2 \tag{6}$$

where α, β and γ are parameters. Since (5) makes $\boldsymbol{V}$ equal to $\boldsymbol{W}^{\mathrm{T}}\boldsymbol{L}$, we could replace one $\boldsymbol{V}$ in (4) with $\boldsymbol{W}^{\mathrm{T}}\boldsymbol{L}$.

3.4 Overall objective function

By combining (3) and (6), the overall objective function can be given as follows:

$$\begin{aligned}\min_{\boldsymbol{P},\boldsymbol{W},\boldsymbol{V}} &\alpha\left\|\boldsymbol{S}-\boldsymbol{V}^{\mathrm{T}}\boldsymbol{W}^{\mathrm{T}}\boldsymbol{L}\right\|_F^2+\beta\left\|\boldsymbol{V}-\boldsymbol{W}^{\mathrm{T}}\boldsymbol{L}\right\|_F^2+\gamma\|\boldsymbol{W}\|_F^2+\\ &\theta\|\boldsymbol{V}-\boldsymbol{P}\boldsymbol{X}\|_F^2+\delta\left\|\boldsymbol{X}-\boldsymbol{P}^{\mathrm{T}}\boldsymbol{V}\right\|_F^2+\eta\|\boldsymbol{P}\|_F^2\\ &\text{s.t. } \boldsymbol{V}\boldsymbol{V}^{\mathrm{T}}=n\boldsymbol{I}_r,\quad \boldsymbol{V}\boldsymbol{1}_n=\boldsymbol{0}_r\end{aligned} \tag{7}$$

where $\boldsymbol{I}_r\in\mathbf{R}^{r\times r}$ denotes the identity matrix, r is the dimension of the latent representation, $\boldsymbol{1}_n$ is all ones column vector, and $\boldsymbol{0}_r$ is all zeros column vector. Here, we further impose the orthogonality and balancedness constraint on $\boldsymbol{V}$ to enhance the discriminative capability of the learned representation. Note that, although (7) involves the large $n\times n$ pairwise similarity matrix $\boldsymbol{S}$, we in fact use $\boldsymbol{G}^{\mathrm{T}}\boldsymbol{G}$ instead of $\boldsymbol{S}$ in optimization to avoid the square complexity of memory and time.

3.5 Optimization

To solve the optimization problem in (7), we propose an alternating optimization algorithm by the following steps.

Step 1. Update $\boldsymbol{P}$. When $\boldsymbol{V}$ and $\boldsymbol{W}$ are fixed, (7) can be rewritten as

$$\min_{\boldsymbol{P}} \theta\|\boldsymbol{V}-\boldsymbol{P}\boldsymbol{X}\|_F^2+\delta\left\|\boldsymbol{X}-\boldsymbol{P}^{\mathrm{T}}\boldsymbol{V}\right\|_F^2+\eta\|\boldsymbol{P}\|_F^2. \tag{8}$$

We set the gradient of the objective function with respect to $\boldsymbol{P}$ to zero, and the solution of $\boldsymbol{P}$ can easily be obtained as follows:

$$\boldsymbol{P}=(\theta+\delta)\boldsymbol{V}\boldsymbol{X}^{\mathrm{T}}(\theta\boldsymbol{X}\boldsymbol{X}^{\mathrm{T}}+(\delta+\eta)\boldsymbol{I})^{-1}. \tag{9}$$

Step 2. Update $\boldsymbol{W}$. We can hold the other variables unchanged to learn $\boldsymbol{W}$. The objective function can be rewritten as

$$\min_{\boldsymbol{W}} \alpha\left\|\boldsymbol{S}-\boldsymbol{V}^{\mathrm{T}}\boldsymbol{W}^{\mathrm{T}}\boldsymbol{L}\right\|_F^2+\beta\left\|\boldsymbol{V}-\boldsymbol{W}^{\mathrm{T}}\boldsymbol{L}\right\|_F^2+\gamma\|\boldsymbol{W}\|_F^2. \tag{10}$$

Analogous to $\boldsymbol{P}$, we set the derivative of the objective with respect to $\boldsymbol{W}$ to zero, and the closed-form solution

of $\boldsymbol{W}$ can be obtained

$$\boldsymbol{W} = ((\alpha+\beta)\boldsymbol{L}\boldsymbol{L}^{\mathrm{T}} + \gamma\boldsymbol{I})^{-1}(\alpha\boldsymbol{L}\boldsymbol{S}^{\mathrm{T}}\boldsymbol{V}^{\mathrm{T}} + \beta\boldsymbol{L}\boldsymbol{V}^{\mathrm{T}}). \quad (11)$$

Step 3. Update $\boldsymbol{V}$. To learn the latent representation $\boldsymbol{V}$, by holding the other variables unchanged, the objective function to solve $\boldsymbol{V}$ can be rewritten as

$$\begin{aligned}\min_{\boldsymbol{V}} \ & \alpha\left\|\boldsymbol{S} - \boldsymbol{V}^{\mathrm{T}}\boldsymbol{W}^{\mathrm{T}}\boldsymbol{L}\right\|_F^2 + \beta\left\|\boldsymbol{V} - \boldsymbol{W}^{\mathrm{T}}\boldsymbol{L}\right\|_F^2 + \\ & \theta\left\|\boldsymbol{V} - \boldsymbol{P}\boldsymbol{X}\right\|_F^2 + \delta\left\|\boldsymbol{X} - \boldsymbol{P}^{\mathrm{T}}\boldsymbol{V}\right\|_F^2 \\ & \text{s.t.} \ \ \boldsymbol{V}\boldsymbol{V}^{\mathrm{T}} = n\boldsymbol{I}_r, \quad \boldsymbol{V}\boldsymbol{1}_n = \boldsymbol{0}_r. \end{aligned} \quad (12)$$

To solve the above problem, we first transform (12) into a matrix trace form with the constrains of $\boldsymbol{V}\boldsymbol{V}^{\mathrm{T}} = n\boldsymbol{I}_r$, and it can be rewritten as

$$\begin{aligned}\max_{\boldsymbol{V}} \ & Tr(((\theta+\delta)\boldsymbol{P}\boldsymbol{X} + \alpha\boldsymbol{W}^{\mathrm{T}}\boldsymbol{L}\boldsymbol{S}^{\mathrm{T}} + \beta\boldsymbol{W}^{\mathrm{T}}\boldsymbol{L})\boldsymbol{V}^{\mathrm{T}}) \\ & \text{s.t.} \ \ \boldsymbol{V}\boldsymbol{V}^{\mathrm{T}} = n\boldsymbol{I}_r, \quad \boldsymbol{V}\boldsymbol{1}_n = \boldsymbol{0}_r. \end{aligned} \quad (13)$$

We define $\boldsymbol{Z} = (\theta+\delta)\boldsymbol{P}\boldsymbol{X} + \alpha\boldsymbol{W}^{\mathrm{T}}\boldsymbol{L}\boldsymbol{S}^{\mathrm{T}} + \beta\boldsymbol{W}^{\mathrm{T}}\boldsymbol{L}$, $\boldsymbol{J} = \boldsymbol{I}_n - (1/n)\boldsymbol{1}_n\boldsymbol{1}_n^{\mathrm{T}}$. The problem can be solved by using the eigendecomposition in $\boldsymbol{Z}\boldsymbol{J}\boldsymbol{Z}^{\mathrm{T}}$ as follows:

$$\boldsymbol{Z}\boldsymbol{J}\boldsymbol{Z}^{\mathrm{T}} = \begin{bmatrix}\boldsymbol{Q} & \tilde{\boldsymbol{Q}}\end{bmatrix}\begin{bmatrix}\boldsymbol{\Omega} & \boldsymbol{0} \\ \boldsymbol{0} & \boldsymbol{0}\end{bmatrix}\begin{bmatrix}\boldsymbol{Q} & \tilde{\boldsymbol{Q}}\end{bmatrix}^{\mathrm{T}} \quad (14)$$

where $\boldsymbol{Q} \in \mathbf{R}^{r\times r'}$ is the corresponding eigenvectors, $\tilde{\boldsymbol{Q}} \in \mathbf{R}^{r\times(r-r')}$ is the matrix of the remaining $r-r'$ eigenvectors, corresponding to zero eigenvalues. $\boldsymbol{\Omega} \in \mathbf{R}^{r'\times r'}$ is the diagonal matrix of positive eigenvalues, and r' is the rank of $\boldsymbol{Z}\boldsymbol{J}\boldsymbol{Z}^{\mathrm{T}}$. Then we can obtain an orthogonal matrix $\bar{\boldsymbol{Q}} \in \mathbf{R}^{r\times(r-r')}$ by conducting a Gram-Schmidt process on $\tilde{\boldsymbol{Q}}$. Furthermore, we define $\boldsymbol{U} = \boldsymbol{J}\boldsymbol{Z}^{\mathrm{T}}\boldsymbol{Q}\boldsymbol{\Omega}^{-1/2}$ and a random orthogonal matrix $\bar{\boldsymbol{U}} \in \mathbf{R}^{n\times(r-r')}$. If $r' = r$, $\bar{\boldsymbol{U}}$, $\bar{\boldsymbol{Q}}$, and $\tilde{\boldsymbol{Q}}$ are empty. Ultimately, the optimal solution for (13) is obtained as follows:

$$\boldsymbol{V} = \sqrt{n}\begin{bmatrix}\boldsymbol{Q} & \bar{\boldsymbol{Q}}\end{bmatrix}\begin{bmatrix}\boldsymbol{U} & \overline{\boldsymbol{U}}\end{bmatrix}^{\mathrm{T}}. \quad (15)$$

By the above steps, we can update all the variables and repeat the process iteratively until the objective function converges. Finally, to show the overall view of the optimization, we summarize it in Algorithm 1.

Algorithm 1. Optimization algorithm

Input: Base feature matrix of training data $\boldsymbol{X}$, parameters α, β, θ, δ, η, γ, and the total iteration number t.

Output: Projection matrix $\boldsymbol{P}$.

Procedure:

Randomly initialize $\boldsymbol{P}$, $\boldsymbol{W}$, $\boldsymbol{V}$;

for $i = 1$ to t> **do**

Update $\boldsymbol{P}$ with (9);

Update $\boldsymbol{W}$ with (11);

Update $\boldsymbol{V}$ with (15);

end for

Return: $\boldsymbol{P}$.

3.6 Convergence analysis

To further comprehend our method, we give a theoretical convergence analysis for our model. Denote $\mathcal{L}(\boldsymbol{P}, \boldsymbol{W}, \boldsymbol{V})$ as the whole objective function. As shown before, there is a closed-form solution for each variable in the corresponding sub-problem, and we have $\mathcal{L}(\boldsymbol{P}^{t+1}, \boldsymbol{W}^{t+1}, \boldsymbol{V}^{t+1}) \leq \mathcal{L}(\boldsymbol{P}^{t+1}, \boldsymbol{W}^{t+1}, \boldsymbol{V}^{t}) \leq \mathcal{L}(\boldsymbol{P}^{t+1}, \boldsymbol{W}^{t}, \boldsymbol{V}^{t}) \leq \mathcal{L}(\boldsymbol{P}^{t}, \boldsymbol{W}^{t}, \boldsymbol{V}^{t})$, which illustrates that the objective loss is monotonously decreasing in each iteration. In addition, $\mathcal{L}(\boldsymbol{P}^{t}, \boldsymbol{W}^{t}, \boldsymbol{V}^{t})$ is bounded below owing to its three positive terms. According to the bounded monotone convergence theorem[35], our method will converge to a local optimal solution. We will plot the convergence curves for better demonstration in our experiments.

3.7 Matching

After the training procedure, the projection matrix $\boldsymbol{P}$ can be learned, which is used to reconstruct the discriminative representations for query samples and enroll samples, represented by $\boldsymbol{P}\boldsymbol{X}^{query}$ and $\boldsymbol{P}\boldsymbol{X}^{enroll}$, respectively. In the matching stage, for each heartbeat vector of the query samples, $y = \boldsymbol{P}\boldsymbol{X}_i^{query}$. We can compute the Euclidean distance among y and enroll samples $y_j^* = \boldsymbol{P}\boldsymbol{X}_j^{enroll}$ $(j = 1, \cdots, c)$ as a measure of their similarity, where c is the number of subjects. If the distance between y and y_j^* is the smallest, the query sample y belongs to the jth subject:

$$Subject(y) = \arg\min_{j=1,\cdots,c}\sqrt{(\boldsymbol{y} - \boldsymbol{y}_{\boldsymbol{j}}^*)^2}. \quad (16)$$

4 Experiments

4.1 Datasets and experimental settings

CYBHiDB[19] is acquired from the palms and fingertips, which is regarded as a challenging off-the-person dataset. In this paper, we used the signals in the long-term, and it contains 63 healthy participants, collected from two sessions with three-month intervals, and we called them T1 and T2, respectively. MIT-BIH[18] is one of the most widely used datasets for ECG biometrics, and it is available in the Physionet[36] repository. It contains 48 two-channel ECG recordings from 47 subjects. Physikalisch-Technische Bundesanstalt (PTB) diagnostic ECG database (PTB)[37] includes 549 recordings from 290 subjects collected using conventional 12 leads together

with the 3 Frank leads. In this paper, we choose 248 subjects whose range is longer than 100 s, and each subject has one recording.

In the heartbeat segmentation stage, we detect the R peak with Pan-Tompkins[38], taking 299 sampling points forward from the R peak and 300 sampling points backward, and a total of 600 sampling points as a heartbeat on CYBHiDB. For MIT-BIH, we take 100 sampling points before the location of R and 159 sampling points after the location of R, with 260 sampling points in one heartbeat. For PTB, there are 460 sampling points in one heartbeat. Then we extracted 1DMRLBP as a base feature, which served as the input of our framework. Each individual has nine homologous samples in the training set and five homologous samples in the testing set. The dimension of the latent representation r is set to 90 and 600 in MIT-BIH and CYBHiDB, respectively. The trade-off parameters, α, β, θ, δ, η, and γ are selected by a validation procedure in the experiment. The convergence of the optimization algorithm is also validated in the experiments.

4.2 Evaluation metrics

We employed the widely used criteria equal error rate (EER) to evaluate the performance in verification mode and EER is the point where false rejection rate (FRR) is equal to the false acceptance rate (FAR). For the identification mode, the accuracy is used as the evaluation criteria, which is the percentage of correctly identified testing samples.

4.3 Comparison with state-of-the-art

We compared the performance of our method with several state-of-the-art methods on MIT-BIH, including non-deep methods[4, 15, 39] and deep learning-based methods[32, 40, 41]. For all baselines, the results are copied from their original papers. The experimental results are summarized in Table 1, and we have the following observations: 1) Our method outperforms all non-deep baselines in MIT-BIH, demonstrating its effectiveness for ECG biometrics. One reason is that our model can better extract semantic information because of the elaborate design of semantic-rich information preserving. The other reason is that our model constructs an enhanced correlation between the base feature and latent representation, reinforcing the discriminative capability of learned representation. Therefore, compared with other traditional non-deep methods, it is able to generate a more discriminative representation. 2) Compared to deep-learning methods, our model achieves comparable performance. The deep model[41] uses 1D-CNN together with attention Bi-LSTM for identification, where it achieves satisfying performance at the cost of much more training time. Especially, our method is superior to these two deep baselines[32, 40] on both accuracy and EER. Therefore, our method can achieve competitive or even superior performance on ECG biometric recognition.

We also conducted the experiments on the challenging off-the-person dataset CYBHiDB in two situations, i.e., within-session and across-session. The experiments in within-session situation use training data and testing data in the same session. For the across-session situation, training data and testing data come from different sessions, where the training data come from the T1 session, while testing data come from the T2 session or training data are from T2 and testing data are from the T1. The baselines for CYBHiDB include non-deep methods[3, 7, 42, 43] and deep method[44]. The experimental results are summarized in Tables 2 and 3. For all baselines, the results are those reported in previous work[7]. From Table 2, we can observe that our model achieves the best accuracy in the within-session for identification mode. For the verification mode, our model achieves competitive EER results. The baseline[7] obtains a better EER because it fused three features (shape, 1dlbp, and wavelet). The deep learning method[44] gets satisfying EER in verification mode, while the accuracy in identification mode is insignificant and time-consuming. For the across-session situation, the experimental results are summarized in Table 3. It is worth noting that our model achieves satisfying performance on both accuracy and EER. The main reason is that our model can preserve semantic informa-

Table 1 Performance analysis on MIT-BIH

Dataset	Method	EER (%)	Accuracy (%)
MIT-BIH	Hejazi et al.[4]	–	98.2
	Wang et al.[15]	2.73	94.68
	Salloum and Kuo[32]	1.37	99.08
	Dar et al.[39]	–	93.1
	Abdeldayem and Bourlai[40]	–	96.5
	Wu et al.[41]	0.02	99.7
	Ours	1.06	99.1

Table 2 Within-session analysis on CYBHiDB

Dataset	Method	EER (%)		Accuracy (%)	
		T1	T2	T1	T2
CYBHiDB	Chan et al.[3]	10.58	11.34	89.16	88.45
	Huang et al.[7]	1.26	2.28	97.43	95.32
	Islam and Alajlan[42]	5.45	6.53	93.52	91.41
	Odinaka et al.[43]	3.12	4.53	95.51	93.26
	Da Silva Luz et al.[44]	1.85	3.35	97.12	94.95
	Ours	3.17	3.70	98.4	96.8

Table 3 Across-session analysis on CYBHiDB

Method	Training	Testing	EER (%)	Accuracy (%)
Chan et al.[3]	T1	T2	20.47	76.11
	T2	T1	18.29	79.38
Huang et al.[7]	T1	T2	10.26	87.75
	T2	T1	11.14	86.24
Islam and Alajlan[42]	T1	T2	15.23	82.49
	T2	T1	14.78	83.83
Odinaka et al.[43]	T1	T2	14.04	83.23
	T2	T1	13.18	84.35
Da Silva Luz et al.[44]	T1	T2	12.78	85.46
	T2	T1	12.83	84.46
Ours	T1	T2	6.17	92.86
	T2	T1	5.86	96.03

tion well and enhance the correlation between the base feature and latent representation. In this respect, it further corroborates the effectiveness of our approach.

Besides, we conducted experiments on PTB, and the baselines include deep learning-based methods[33, 41] and non-deep methods[7, 45, 46]. Experimental results are summarized in Table 4. For all baselines, the results are those reported in previous work[45]. From Table 4, we can observe that our method outperforms all non-deep baselines and achieves comparable accuracy compared with deep-learning methods. In other words, our method outperforms (or is in part with) existing methods. Taking into account both performance and efficiency, our proposed method may be the most practical.

Table 4 Performance analysis on PTB

Dataset	Method	Accuracy (%)
PTB	Huang et al.[7]	98.02
	Zhao et al.[33]	98.62
	Wu et al.[41]	98.86
	Huang et al.[45]	98.19
	Louis et al.[46]	98.18
	Ours	98.59

4.4 Parameters sensitive analysis

In this section, we conducted experiments to analyze the sensitivity of parameters including α, β, θ, δ, η, and γ. We recorded the accuracy on MIT-BIH and CYBHiDB by varying all of them in the range of $[0.001, 1000]$, and the results are plotted in Fig. 1. We can observe that some parameters are not sensitive, and we set α, β, and γ to 1. When the value of η increases from 0.001 to 1, the accuracy is generally maintained satisfactory. For the parameter θ, the performance improves when it ranges from 0.1 to 1. Furthermore, our model achieves the best results when δ ranges from 0.01 to 1. Thus, we set $\eta = 1$, $\theta = 0.1$ and $\delta = 0.1$ in our experiment, respectively.

In a nutshell, although there are several parameters in our framework, most of them are not sensitive and could

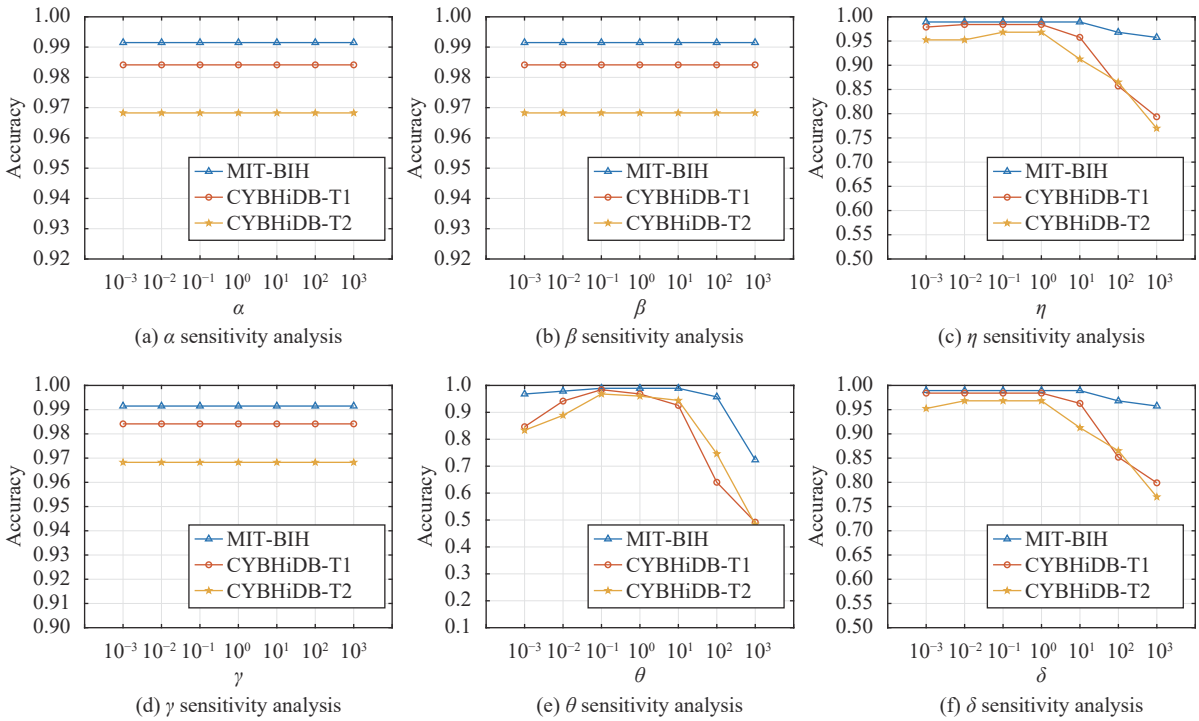

(a) α sensitivity analysis (b) β sensitivity analysis (c) η sensitivity analysis

(d) γ sensitivity analysis (e) θ sensitivity analysis (f) δ sensitivity analysis

Fig. 1 Balance parameter analysis

be easily tuned in practice.

4.5 Time cost analysis

In this section, we summarize the feature extraction time and matching time on MIT-BIH to verify the efficiency of our method. The results are reported in Table 5, and we compute the average feature extraction time per sample and the average matching time per sample pair repeated 20 times. Table 5 shows that our method consumes less time no matter the process of feature extraction or matching procedure, and we can conclude that our method is efficient.

Table 5 Comparison of time costs on MIT-BIH

Method	Feature extraction time (s)	Matching time (s)
Wang et al.[15]	0.008	0.002
Li et al.[16]	0.091 4	0.007
Ours	0.004 6	0.001 6

4.6 Ablation analysis

In this section, we conducted ablation experiments on MIT-BIH to investigate the effectiveness of enhanced correlation and semantic-rich embedding, separately. In particular, we design a variant of our method called OURS_1 by setting $\delta = 0$ to validate the contributions of enhanced correlation. We design another variant of our method called OURS_2 by setting $\beta = 0$ to eliminate the influence of semantic-rich embedding. The experimental results of our method and its variants on MIT-BIH are reported in Table 6. From Table 6, it can be seen that the accuracy of our method outperforms OURS_1 and OURS_2, demonstrating the significance of the enhanced correlation and semantic-rich embedding for ECG biometrics.

4.7 Convergence analysis

In Section 3.6, we proved that the iterative optimization is convergent, and we further conducted experiments to investigate the convergence on two datasets. Specifically, we recorded the accuracy as the iteration increased, and the convergence curves are plotted in Fig. 2. As shown in Fig. 2, the optimization algorithm converges very fast, and the performance increases and tends to be stable after several iterations within five iterations on two datasets, thereby distinctly saving the time required for training.

Table 6 Ablation experiments on MIT-BIH

Method	Accuracy (%)
OURS_1	95.74
OURS_2	96.28
Ours	99.1

5 Conclusions

In this paper, we propose a new framework for ECG biometrics based on constructing enhanced correlation and embedding semantic-rich information. Firstly, the correlation between the base feature and latent representation can be constructed, and we further enhance the correlation by formulating the bidirectional projections with one matrix. Secondly, we design an asymmetric loss function, which includes both the label matrix and the pairwise similarity among the samples, to embed the semantic-rich information into the learning of latent representation for the ECG signal. Then, we combine both enhanced correlation and semantic-rich embedding together to derive the final objective loss and propose an effective algorithm to optimize it. Extensive experiments on two widely-used datasets demonstrate that the proposed framework outperforms the state-of-the-art. In future work, we will explore online ECG biometrics to handle incremental datasets with new instances.

Acknowledgements

This work was supported by National Natural Science Foundation of China (No. 62076151), Natural Science Foundation of Shandong Province, China (No. ZR2020 MF052), and the NSFC-Xinjiang Joint Fund, China (No.

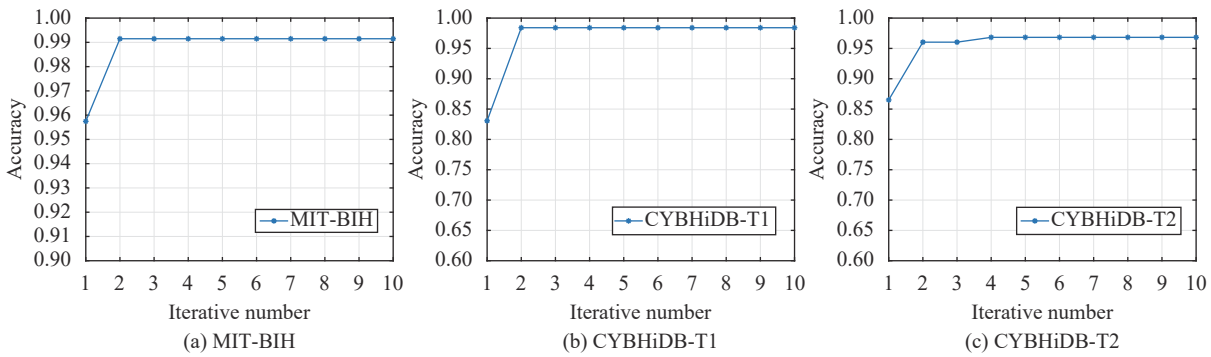

(a) MIT-BIH (b) CYBHiDB-T1 (c) CYBHiDB-T2

Fig. 2 Convergence analysis

U1903127).

Declarations of conflict of interest

The authors declared that they have no conflicts of interest to this work.

References

[1] S. A. El Rahman. Biometric human recognition system based on ECG. *Multimedia Tools and Applications*, vol. 78, no. 13, pp. 17555–17572, 2019. DOI: 10.1007/s11042-019-7152-0.

[2] Y. N. Singh, P. Gupta. ECG to individual identification. In *Proceedings of the 2nd IEEE International Conference on Biometrics: Theory, Applications and Systems*, IEEE, Washington DC, USA, 2008. DOI: 10.1109/BTAS.2008.4699343.

[3] A. D. C. Chan, M. M. Hamdy, A. Badre, V. Badee. Wavelet distance measure for person identification using electrocardiograms. *IEEE Transactions on Instrumentation and Measurement*, vol. 57, no. 2, pp. 248–253, 2008. DOI: 10.1109/TIM.2007.909996.

[4] M. Hejazi, S. A. R. Al-Haddad, S. J. Hashim, A. F. A. Aziz, Y. P. Singh. Feature level fusion for biometric verification with two-lead ECG signals. In *Proceedings of the 12th International Colloquium on Signal Processing & its Applications*, IEEE, Melaka, Malaysia, pp. 54–59, 2016. DOI: 10.1109/CSPA.2016.7515803.

[5] K. N. Plataniotis, D. Hatzinakos, J. K. M. Lee. ECG biometric recognition without fiducial detection. In *Proceedings of Biometrics Symposium: Special Session on Research at the Biometric Consortium Conference*, IEEE, Baltimore, USA, 2006. DOI: 10.1109/BCC.2006.4341628.

[6] R. Balasubramanian, T. Chaspari, S. S. Narayanan. A knowledge-driven framework for ECG representation and interpretation for wearable applications. In *Proceedings of IEEE International Conference on Acoustics, Speech and Signal Processing*, New Orleans, USA, pp. 1018–1022, 2017. DOI: 10.1109/ICASSP.2017.7952310.

[7] Y. W. Huang, G. P. Yang, K. K. Wang, H. Y. Liu, Y. L. Yin. Learning joint and specific patterns: A unified sparse representation for off-the-person ECG biometric recognition. *IEEE Transactions on Information Forensics and Security*, vol. 16, pp. 147–160, 2021. DOI: 10.1109/TIFS.2020.3006384.

[8] J. X. Xu, G. P. Yang, K. K. Wang, Y. W. Huang, H. Y. Liu, Y. L. Yin. Structural sparse representation with class-specific dictionary for ECG biometric recognition. *Pattern Recognition Letters*, vol. 135, pp. 44–49, 2020. DOI: 10.1016/j.patrec.2020.04.022.

[9] L. Kanaan, D. Merheb, M. Kallas, C. Francis, H. Amoud, P. Honeine. PCA and KPCA of ECG signals with binary SVM classification. In *Proceedings of the IEEE Workshop on Signal Processing Systems*, Beirut, Lebanon, pp. 344–348, 2011. DOI: 10.1109/SiPS.2011.6089000.

[10] R. J. Martis, U. R. Acharya, L. C. Min. ECG beat classification using PCA, LDA, ICA and discrete wavelet transform. *Biomedical Signal Processing and Control*, vol. 8, no. 5, pp. 437–448, 2013. DOI: 10.1016/j.bspc.2013.01.005.

[11] S. C. Wu, P. Z. Chen, A. L. Swindlehurst, P. L. Hung. Cancelable biometric recognition with ECGs: Subspace-based approaches. *IEEE Transactions on Information Forensics and Security*, vol. 14, no. 5, pp. 1323–1336, 2019. DOI: 10.1109/TIFS.2018.2876838.

[12] I. Odinaka, P. H. Lai, A. D. Kaplan, J. A. O'Sullivan, E. J. Sirevaag, J. W. Rohrbaugh. ECG biometric recognition: A comparative analysis. *IEEE Transactions on Information Forensics and Security*, vol. 7, no. 6, pp. 1812–1824, 2012. DOI: 10.1109/TIFS.2012.2215324.

[13] K. K. Wang, G. P. Yang, L. Yang, Y. W. Huang, Y. L. Yin. STERLING: Towards effective ECG biometric recognition. In *Proceedings of IEEE International Joint Conference on Biometrics*, Shenzhen, China, 2021. DOI: 10.1109/IJCB52358.2021.9484360.

[14] K. K. Wang, G. P. Yang, Y. W. Huang, L. Yang, Y. L. Yin. Joint dual-domain matrix factorization for ECG biometric recognition. In *Proceedings of IEEE International Conference on Acoustics, Speech and Signal Processing*, Singapore, pp. 3134–3138, 2022. DOI: 10.1109/ICASSP43922.2022.9746066.

[15] K. K. Wang, G. P. Yang, Y. W. Huang, Y. L. Yin. Multi-scale differential feature for ECG biometrics with collective matrix factorization. *Pattern Recognition*, vol. 102, Article number 107211, 2020. DOI: 10.1016/j.patcog.2020.107211.

[16] R. Li, G. P. Yang, K. K. Wang, Y. W. Huang, F. Yuan, Y. L. Yin. Robust ECG biometrics using GNMF and sparse representation. *Pattern Recognition Letters*, vol. 129, pp. 70–76, 2020. DOI: 10.1016/j.patrec.2019.11.005.

[17] Y. W. Huang, G. P. Yang, K. K. Wang, H. Y. Liu, Y. L. Yin. Robust multi-feature collective non-negative matrix factorization for ECG biometrics. *Pattern Recognition*, vol. 123, Article number 108376, 2022. DOI: 10.1016/j.patcog.2021.108376.

[18] G. B. Moody, R. G. Mark. The impact of the MIT-BIH arrhythmia database. *IEEE Engineering in Medicine and Biology Magazine*, vol. 20, no. 3, pp. 45–50, 2001. DOI: 10.1109/51.932724.

[19] H. P. Da Silva, A. Lourenço, A. Fred, N. Raposo, M. Aires-de-Sousa. Check your biosignals here: A new dataset for off-the-person ECG biometrics. *Computer Methods and Programs in Biomedicine*, vol. 113, no. 2, pp. 503–514, 2014. DOI: 10.1016/j.cmpb.2013.11.017.

[20] J. S. Arteaga-Falconi, H. Al Osman, A. El Saddik. ECG authentication for mobile devices. *IEEE Transactions on Instrumentation and Measurement*, vol. 65, no. 3, pp. 591–600, 2016. DOI: 10.1109/TIM.2015.2503863.

[21] A. Barros, D Rosário, P. Resque, E. Cerqueira. Heart of IoT: ECG as biometric sign for authentication and identification. In *Proceedings of the 15th International Wireless Communications & Mobile Computing Conference*, IEEE, Tangier, Morocco, pp. 307–312, 2019. DOI: 10.1109/IWCMC.2019.8766495.

[22] L. Biel, O. Pettersson, L. Philipson, P. Wide. ECG analysis: A new approach in human identification. *IEEE Transactions on Instrumentation and Measurement*, vol. 50, no. 3, pp. 808–812, 2001. DOI: 10.1109/19.930458.

[23] S. A. Israel, J. M. Irvine, A. Cheng, M. D. Wiederhold, B. K. Wiederhold. ECG to identify individuals. *Pattern Recognition*, vol. 38, no. 1, pp. 133–142, 2005. DOI: 10.1016/j.patcog.2004.05.014.

[24] A. Pal, Y. N. Singh. Biometric recognition using area under curve analysis of electrocardiogram. *International Journal of Advanced Computer Science and Applications*,

vol. 10, no. 1, pp. 533–545, 2019. DOI: 10.14569/IJACSA.2019.0100169.

[25] C. Bück, P. Kovács, P. Laguna, J. Meier, M. Huemer. ECG beat representation and delineation by means of variable projection. *IEEE Transactions on Biomedical Engineering*, vol. 68, no. 10, pp. 2997–3008, 2021. DOI: 10.1109/TBME.2021.3058781.

[26] A. Galli, G. Giorgi, C. Narduzzi. Individual recognition by gaussian ECG features. In *Proceedings of IEEE International Instrumentation and Measurement Technology Conference*, Dubrovnik, Croatia, pp. 1–5, 2020. DOI: 10.1109/I2MTC43012.2020.9129092.

[27] T. N. Alotaiby, S. R. Alrshoud, S. A. Alshebeili, L. M. Aljafar. ECG-based subject identification using statistical features and random forest. *Journal of Sensors*, vol. 2019, Article number 6751932, 2019. DOI: 10.1155/2019/6751932.

[28] W. Louis, D. Hatzinakos. Enhanced binary patterns for electrocardiogram (ECG) biometrics. In *Proceedings of IEEE Canadian Conference on Electrical and Computer Engineering*, Vancouver, Canada, pp. 1–4, 2016. DOI: 10.1109/CCECE.2016.7726725.

[29] M. Hejazi, S. A. R. Al-Haddad, Y. P. Singh, S. J. Hashim, A. F. A. Aziz. ECG biometric authentication based on non-fiducial approach using kernel methods. *Digital Signal Processing*, vol. 52, pp. 72–86, 2016. DOI: 10.1016/j.dsp.2016.02.008.

[30] J. K. Wang, X. Qiao, C. C. Liu, X. P. Wang, Y. Y. Liu, L. K. Yao, H. Zhang. Automated ECG classification using a non-local convolutional block attention module. *Computer Methods and Programs in Biomedicine*, vol. 203, Article number 106006, 2021. DOI: 10.1016/j.cmpb.2021.106006.

[31] G. P. Zhu, M. Z. Ma, Y. W. Huang, K. K. Wang, G. P. Yang. Dual-domain low-rank fusion deep metric learning for off-the-person ECG biometrics. In *Proceedings of IEEE International Conference on Acoustics, Speech and Signal Processing*, Singapore, pp. 2914–2918, 2022. DOI: 10.1109/ICASSP43922.2022.9747122.

[32] R. Salloum, C. C. J. Kuo. ECG-based biometrics using recurrent neural networks. In *Proceedings of IEEE International Conference on Acoustics, Speech and Signal Processing*, Orleans, USA, pp. 2062–2066, 2017. DOI: 10.1109/ICASSP.2017.7952519.

[33] Z. D. Zhao, Y. F. Zhang, Y. J. Deng, X. H. Zhang. ECG authentication system design incorporating a convolutional neural network and generalized S-transformation. *Computers in Biology and Medicine*, vol. 102, pp. 168–179, 2018. DOI: 10.1016/j.compbiomed.2018.09.027.

[34] R. D. Labati, E. Muñoz, V. Piuri, R. Sassi, F. Scotti. Deep-ECG: Convolutional neural networks for ECG biometric recognition. *Pattern Recognition Letters*, vol. 126, pp. 78–85, 2019. DOI: 10.1016/j.patrec.2018.03.028.

[35] W. Rudin. *Principles of Mathematical Analysis*, New York, USA: McGraw-Hill, 1976.

[36] A. L. Goldberger, L. A. Amaral, L. Glass, J. M. Hausdorff, P. C. Ivanov, R. G. Mark, J. E. Mietus, G. B. Moody, C. K. Peng, H. E. Stanley. PhysioBank, physioToolkit, and physioNet: Components of a new research resource for complex physiologic signals. *Circulation*, vol. 101, no. 23, pp. e215–e220, 2000. DOI: 10.1161/01.cir.101.23.e215.

[37] R. Bousseljot, D. Kreiseler, A. Schnabel. Nutzung der EKG-Signaldatenbank CARDIODAT der PTB über das internet. *Biomedizinische Technik/Biomedical Engineering*, vol. 40, no. 1, pp. 317–318, 1995. DOI: 10.1515/bmte.1995.40.s1.317.

[38] J. P. Pan, W. J. Tompkins. A real-time QRS detection algorithm. *IEEE Transactions on Biomedical Engineering*, vol. BME-32, no. 3, pp. 230–236, 1985. DOI: 10.1109/TBME.1985.325532.

[39] M. N. Dar, M. U. Akram, A. Usman, S. A. Khan. ECG biometric identification for general population using multiresolution analysis of DWT based features. In *Proceedings of the 2nd International Conference on Information Security and Cyber Forensics*, IEEE, Cape Town, South Africa, pp. 5–10, 2015. DOI: 10.1109/InfoSec.2015.7435498.

[40] S. S. Abdeldayem, T. Bourlai. A novel approach for ECG-based human identification using spectral correlation and deep learning. *IEEE Transactions on Biometrics, Behavior, and Identity Science*, vol. 2, no. 1, 2020. DOI: 10.1109/TBIOM.2019.2947434.

[41] B. Wu, G. P. Yang, L. Yang, Y. L. Yin. Robust ECG biometrics using two-stage model. In *Proceedings of the 24th International Conference on Pattern Recognition*, IEEE, Beijing, China, pp. 1062–1067, 2018. DOI: 10.1109/ICPR.2018.8545285.

[42] M. S. Islam, N. Alajlan. Biometric template extraction from a heartbeat signal captured from fingers. *Multimedia Tools and Applications*, vol. 76, no. 10, pp. 12709–12733, 2017. DOI: 10.1007/s11042-016-3694-6.

[43] I. Odinaka, P. H. Lai, A. D. Kaplan, J. A. O'Sullivan, E. J. Sirevaag, S. D. Kristjansson, A. K. Sheffeld, J. W. Rohrbaugh. ECG biometrics: A robust short-time frequency analysis. In *Proceedings of IEEE International Workshop on Information Forensics and Security*, Seattle, USA, 2010. DOI: 10.1109/WIFS.2010.5711466.

[44] E. J. Da Silva Luz, G. J. P. Moreira, L. S. Oliveira, W. R. Schwartz, D. Menotti. Learning deep off-the-person heart biometrics representations. *IEEE Transactions on Information Forensics and Security*, vol. 13, no. 5, pp. 1258–1270, 2018. DOI: 10.1109/TIFS.2017.2784362.

[45] Y. W. Huang, G. P. Yang, K. K. Wang, Y. L. Yin. Multi-view discriminant analysis with sample diversity for ECG biometric recognition. *Pattern Recognition Letters*, vol. 145, pp. 110–117, 2021. DOI: 10.1016/J.PATREC.2021.01.027.

[46] W. Louis, M. Komeili, D. Hatzinakos. Continuous authentication using one-dimensional multi-resolution local binary patterns (1DMRLBP) in ECG biometrics. *IEEE Transactions on Information Forensics and Security*, vol. 11, no. 12, pp. 2818–2832, 2016. DOI: 10.1109/TIFS.2016.2599270.

Kui-Kui Wang received the M. Sc. degree in computer science and technology from Shandong University, China in 2017. Currently, she is a Ph. D. degree candidate in software engineering at School of Software Engineering, Shandong University, China.

Her research interests include pattern recognition, biometrics, and machine learning.

E-mail: sarahkuikui@163.com
ORCID iD: 0000-0002-0790-0736

Gong-Ping Yang received the Ph. D. degree in computer software and theory from Shandong University, China in 2007. He is currently a professor at School of Software Engineering, Shandong University, China and an adjunct professor at School of Computer, Heze University, China.

His research interests include pattern recognition, image processing, and biometrics.

E-mail: gpyang@sdu.edu.cn (Corresponding author)
ORCID iD: 0000-0001-7637-2749

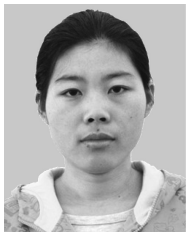

Lu Yang received the Ph. D. degree in computer science and technology from Shandong University, China in 2016. Now she is a professor with School of Computer Science and Technology, Shandong Jianzhu University, China.

Her research interests include biometrics and machine learning.

E-mail: yangluhi@163.com

Yu-Wen Huang received the Ph. D. degree in computer science and technology from Shandong University, China in 2021. Now he is an associate professor with School of Computer, Heze University, China.

His research interests include ECG recognition, biometrics and machine learning.

E-mail: hzxy_hyw@163.com

Yi-Long Yin received the Ph. D. degree in agricultural mechanization engineering from Jilin University, China in 2000. He is the director of the Machine Learning and Data Mining Group and a professor with Shandong University, China. From 2000 to 2002, he was a post-doctoral fellow with Department of Electronic Science and Engineering, Nanjing University, China.

His research interests include machine learning, data mining and computer vision.

E-mail: ylyin@sdu.edu.cn

Machine Intelligence Research

Citation: K. K. Wang, G. P. Yang, L. Yang, Y. W. Huang, Y. L. Yin. Ecg biometrics via enhanced correlation and semantic–rich embedding. *Machine Inteligence Research*, vol.20, no.5, pp.697–706, 2023. https://doi.org/10.1007/s11633–022–1345–0